# Identification of vulnerable carotid plaque with CT-based radiomics nomogram

M. Liu [a], N. Chang [b], S. Zhang [c,d], Y. Du [a], X. Zhang [d], W. Ren [d], J. Sun [d], J. Bai [e], L. Wang [f,**,†], G. Zhang [a,*,†]

[a] *Department of Health Management, The First Affiliated Hospital of Shandong First Medical University, Jinan, China*
[b] *Department of Medical Technology, Jinan Nursing Vocational College, No. 3636 Gangxi Road, Jinan 250021, Shandong, China*
[c] *Shandong Provincial Hospital Affiliated to Shandong First Medical University, Jinan China*
[d] *Postgraduate Department, Shandong First Medical University (Shandong Academy of Medical Sciences), Jinan, China*
[e] *Department of Computed Tomography, Liaocheng Traditional Chinese Medicine Hospital, Liaocheng, China*
[f] *Physical Examination Centre, Shandong Provincial Hospital Affiliated to Shandong First Medical University, Jinan, China*

AIM: To develop and validate a radiomics nomogram for identifying high-risk carotid plaques on computed tomography (CT) angiography (CTA).

MATERIALS AND METHODS: A total of 280 patients with symptomatic ($n=131$) and asymptomatic ($n=139$) carotid plaques were divided into a training set ($n=135$), validation set ($n=58$), and external test set ($n=87$). Radiomic features were extracted from CTA images. A radiomics model was constructed based on selected features and a radiomics score (rad-score) was calculated. A clinical factor model was constructed by demographics and CT findings. A radiomics nomogram combining independent clinical factors and the rad-score was constructed. The diagnostic performance of three models was evaluated and validated by region of characteristic curves.

RESULTS: Calcification and maximum plaque thickness were the independent clinical factors. Twenty-four features were used to build the radiomics signature. In the validation set, the nomogram (area under the curve [AUC], 0.977; 95% CI, 0.899−0.999) performed better ($p=0.017$ and $p=0.031$) than the clinical factor model (AUC, 0.862; 95% CI, 0.746−0.938) and radiomics signature (AUC, 0.944; 95% CI, 0.850−0.987). In external test set, the nomogram (AUC, 0.952; 95% CI, 0.884−0.987) and radiomics signature (AUC, 0.932; 95% CI, 0.857−0.975) showed better discrimination capability ($p=0.002$ and $p=0.037$) than clinical factor model (AUC, 0.818; 95% CI, 0.721−0.892).

* Guarantor and correspondent: G. Zhang, Department of Health Management, The First Affiliated Hospital of Shandong First Medical University, No. 16766 Jingshi Road, Jinan 250014, China. Tel./fax: +86 0531 89268763.
** Guarantor and correspondent: L. Wang, Physical Examination Center, Shandong Provincial Hospital Affiliated to Shandong First Medical University, No. 324, Jingwu Road, Jinan, Shandong 250021, China. Tel./fax: +86 0531 68779172.
E-mail addresses: z6321106@126.com (L. Wang), zgzg2023@yeah.net (G. Zhang).
† These authors contributed equally to this work.

CONCLUSION: The CT-based nomogram showed satisfactory performance in identification of high-risk plaques in carotid arteries, and it may serve as a potential non-invasive tool to identify carotid plaque vulnerability and risk stratification.

© 2023 Published by Elsevier Ltd on behalf of The Royal College of Radiologists.

## Introduction

Atherosclerotic plaque in the carotid artery is a main reason for cerebrovascular disease.[1,2] Nowadays, the global prevalence of carotid atherosclerosis is gradually increasing, which has attracted more attention and research.[3] Based on the utility of stenosis measurement alone to identify ischaemic stroke patients at highest risk, recent studies on medical imaging techniques have attempted to provide a more detailed characterisation of vulnerable plaques.[4,5] Although it is reliable and non-invasive, medical imaging is complicated and requires specialised knowledge in identifying various plaque characteristics. Therefore, the distinction between symptomatic and asymptomatic carotid plaque remains a radiographic diagnostic challenge. Radiomics may serve as a potential tool to improve the accuracy of diagnostic evaluation in identifying vulnerable carotid plaques.

Radiomics is a computational process that extracts and analyses a great quantity of radiomic features from medical images.[6] It has been widely used and is of great value in oncology, including tumour diagnosis, staging, grading, and prognostic evaluation.[7–9] Recently, it was reported that computed tomography (CT) texture-based radiomics analysis has been employed to identify vulnerable plaques and it may act as a novel risk-stratification tool in patients with carotid atherosclerosis.[10] Several studies have reported that radiomics models using magnetic resonance imaging (MRI) can accurately discriminate between symptomatic and asymptomatic carotid plaques.[11] Nevertheless, most studies were focused on radiomics texture analysis, and more radiomics studies with statistical characterisation are required to provide more detailed plaque analysis. To the authors' knowledge, few relevant studies had been performed to identify vulnerable carotid plaques using a CT-based radiomics nomogram.

The purpose of this study was to develop and validate a radiomics nomogram that would incorporate radiomics signatures and clinical factors to identify high-risk carotid plaques.

## Materials and methods

All study procedures were approved by the institutional review board, and informed consent was waived because of the retrospective nature of the study. Consecutive patients who underwent CT angiography (CTA) for suspected carotid atherosclerotic disease from February 2019 to April 2021 at The First Affiliated Hospital of Shandong First Medical University were screened. One hundred and ninety-three patients with symptomatic (*n*=93, 74 men and 19 women; mean age, 63.5 ± 7.1 years) and asymptomatic (*n*=100, 62 men and 38 women; mean age, 64 ± 8.8 years) carotid plaques were enrolled in this study according to the following inclusion criterion: extracranial carotid artery stenosis secondary to atherosclerosis disease on CTA. The exclusions criteria were as follows: (1) history of carotid stenting and endarterectomy; (2) cardiac thrombus; (3) carotid occlusion; (4) CTA images with poor quality; (5) patients who had symptoms occurring in the both carotid supplying territory. The patients were divided into training and validation cohorts according to the proportion of 7:3 by computer-generated random numbers. Eighty-seven patients with symptomatic (*n*=48, 38 men and 10 women; mean age, 62.8 ± 7.5 years) and asymptomatic (*n*=39, 27 men and 12 women; mean age, 63.4 ± 8.6 years) carotid plaques were enrolled as the external test set from another hospital according to the same inclusion and exclusion criteria. A flowchart for selecting the study population is shown in Fig 1.

Patients were classified as symptomatic or asymptomatic according to the neurological assessment.[12] A symptomatic patient was considered a patient with a stroke or transient ischaemic attack (TIA) occurring in the carotid supplying territory. Stroke was defined as permanent neurological dysfunction by focal brain or retinal ischaemia.[13] TIA was defined as a transient episode of neurological dysfunction by focal brain or retinal ischaemia.[13] Patients were considered as asymptomatic if they had no cerebrovascular symptoms in the past 6 months.

Demographic and clinical data including age, sex, body mass index, hypertension, hyperlipidaemia, diabetes, smoking, coronary artery disease, anti-hypertensive drug use, statin use, and anti-platelet use were collected from medical record.

### CTA protocol

CTA was performed using a third-generation dual-source CT system (SOMATOM Force; Siemens Healthineers, Erlangen, Germany). A 70−90 ml volume of contrast media (Omnipaque-350; GE Healthcare, New Jersey, USA) was injected using a power injector at a rate of 5−6 ml/s, followed by 50 ml of saline flush. Acquisition was triggered using bolus tracking after reaching an attenuation threshold of 100 HU in the aortic arch for 5 seconds.

The carotid CTA parameters were as follows: tube voltage of 110 kVp, pitch of 1.0, reconstructed section interval of 0.5 mm, reconstructed section thickness of 0.5 mm and rotation time of 400 ms. CTA studies were obtained in helical scanning mode, and scanning extended from the aortic arch to the cranial vertex.
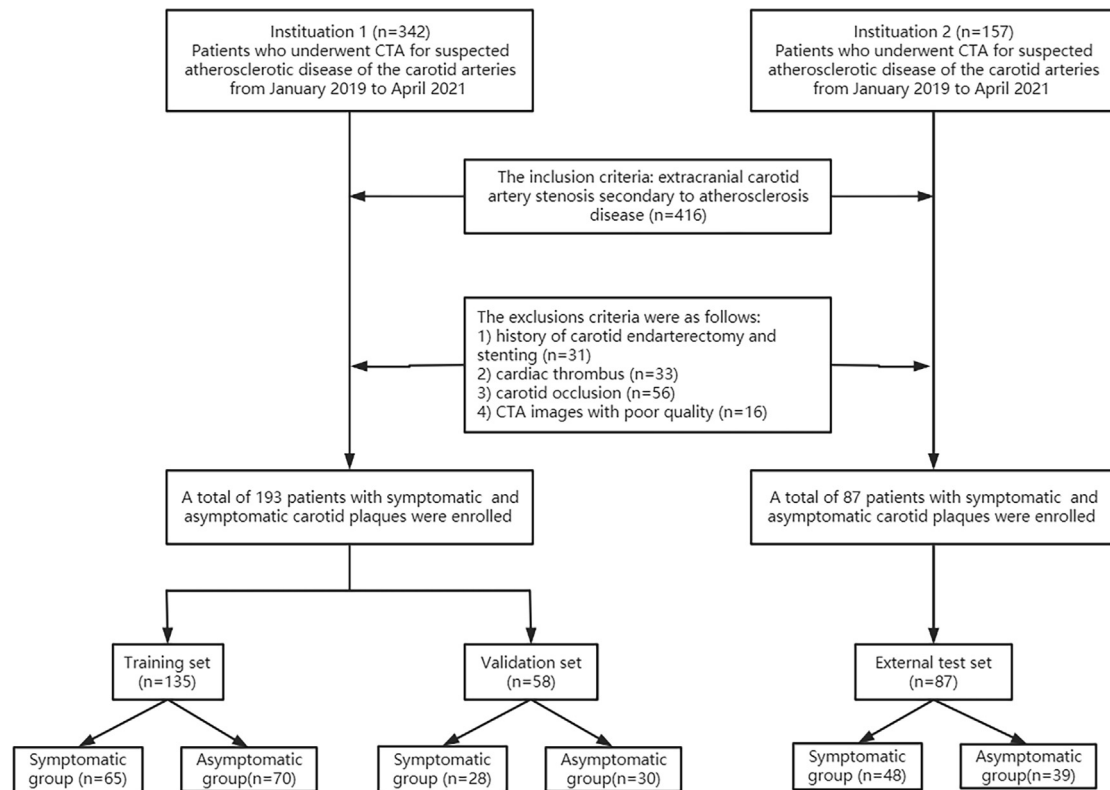
**Figure 1** Flowchart of patients' collection pathway.

*CTA image analysis*

The measurements of CTA markers (presence of calcification, maximum plaque thickness, and degree of luminal stenosis) were obtained using post-processing workstation (Syngo.via, Siemens, Germany). The degree of stenosis was determined in accordance with the North American Symptomatic Carotid Endarterectomy Trial (NASCET) criteria on CTA.[14] All CTA images were independently assessed by two radiologists with more than 8 years' experience in medical imaging, both of whom were blinded to patient clinical information and had any disagreements in evaluation resolved by consensus.

*Development of the clinical factor model*

Univariable analysis was applied to compare the differences in the clinical factors (including clinical data and CTA features) in the training, validation, and external test cohorts. Then, a multivariable logistic regression analysis was used to build the clinical factor model. Odds ratios (OR) as estimates of relative risk with 95% confidence intervals (CIs) were calculated for each independent factor.

*Development of the radiomics signature and radiomics nomogram*

Plaque segmentation was performed on the CTA images using ITK-SNAP software (version 3.7). The regions of interests (ROIs) were segmented manually in the cross-

sectional area of the plaque. Contours were drawn within the borders of the plaque, and care was taken not to include the adjacent normal tissue. Feature extraction was performed using the Radcloud platform (Huiying Medical Technology, Beijing, China). A total of 234 radiomic features were extracted from the medical imaging. The details of the radiomic features are shown in Electronic Supplementary Material Table S1. The inter- and intra-class correlation coefficients (ICCs) were used to evaluate the interobserver and intraobserver reproducibility of feature extraction. CTA images of 20 cases (seven symptomatic plaques and 13 asymptomatic plaques) were selected randomly to perform ROI segmentation by radiologists 1 and 2. Radiologist 1 repeated the segmentation 3 weeks later to assess the reproducibility of extraction. An ICC >0.75 indicates good agreement of the feature extraction. Then the remaining image segmentation was performed by radiologist 1.

To avoid dimensionality distortions and reduces biases of radiomic features during modelling, dimension reduction of the properties was conducted before signature construction. Briefly, the radiomic features with ICCs >0.75 were underwent one-way analysis of variance (ANOVA) to choose potential significant features. Then the select_k_best method was performed to eliminate the redundant and irrelevant features. The remaining features were then included in a least absolute shrinkage and selection operator (LASSO) regression model to choose the most significant characteristics in the training cohort. Then, the selected features were applied to build a radiomics signature. A radiomics score (rad-score) was computed for all
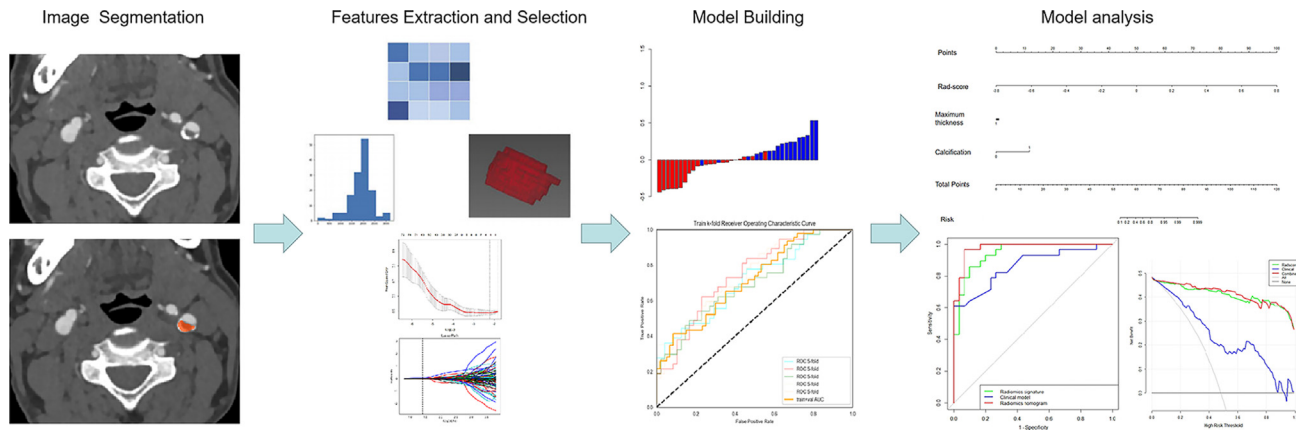
**Figure 2** The overall workflow of the radiomics model development.

patients using significant features selected by LASSO coefficients.

A radiomics nomogram was constructed by incorporating the significant variables of the clinical factors and the rad-score. The radiomics nomogram included the same features of the radiomics signature. The goodness-of-fit of the nomogram was evaluated using the Hosmer–Lemeshow test and calibration curves. The workflow of the development of the radiomics model is displayed in Fig 2.

### Assessment of the performance of different models

The diagnostic performance of the clinical factor model, the radiomics model, and the radiomics nomogram model for distinguishing symptomatic and asymptomatic carotid plaques were assessed from the area under the curve (AUC) of the receiver operator characteristic (ROC) curve in the training, validation, and external test cohorts. To evaluate the clinical value of the nomogram model, decision curve analysis (DCA) was performed by calculating the net benefits for a range of threshold probabilities in the training, validation, and external test cohorts.

### Statistical analysis

Continuous variables are described as mean ± standard deviation (SD), and categorical variables are presented as percentages. Univariable analysis was used to compare differences in the clinical factors between the two patient groups, using independent samples *t*-tests for quantitative data, and the chi-square or Fisher's exact tests for qualitative data, as appropriate. One-way ANOVA was performed to compare with each radiomics signature for the differentiation of symptomatic and asymptomatic carotid plaques. The LASSO regression was applied using the "glmnet" package. ROC curves were plotted using the "pROC" package. Distinctions in AUC values among different models were estimated using the Delong test. Nomogram development and calibration curves were performed using the "rms" package. DCA was applied using the "rmda" package. The Hosmer–Lemeshow test was employed using the "generalhoslem" package. Statistical significance was considered at

$p<0.05$. Statistical analysis was performed using SPSS (version 22.0, IBM, Armonk, NY, USA) and R statistical software (version 3.3.3, https://www.r-project.org).

## Results

The clinical characteristics of the patients in the training, validation, and external test sets are summarised in Table 1. Sex, hyperlipidaemia, calcification, degree of luminal stenosis, and maximum plaque thickness showed significant differences in the training cohort ($p<0.05$). The multivariable logistic regression analysis suggested that only calcification and maximum plaque thickness remained as independent predictors. Compared with asymptomatic patients, those symptomatic patients showed a higher prevalence of calcification (OR, 58.26; 95% confidence interval [CI], 4.17–815.60; $p=0.003$) and greater maximum plaque thickness (OR, 2.62; 95% CI, 1.47–4.68; $p=0.001$).

Of the 234 radiomic features collected from the CTA images, 221 had good inter- and intraobserver agreement, with ICCs >0.75; 117 radiomic features showed significant differences between symptomatic and asymptomatic carotid plaques by ANOVA. Among the 117 radiomic features, 93 stable radiomic features were retained by the select_k_best method. These features were then used to select the most valuable features by LASSO. Twenty-four features were finally used to build the radiomics signature. According to these features, rad-score calculation is shown in Electronic Supplementary Material Equation S1. A significant distinction was found in the rad-score between the symptomatic and asymptomatic groups in the training set ($0.30 \pm 0.24$ versus $-0.28 \pm 0.22$; $p<0.001$), which was then confirmed in the validation set ($0.40 \pm 0.22$ versus $-0.34 \pm 0.18$; $p<0.001$), and the external test set ($0.31 \pm 0.22$ versus $-0.15 \pm 0.26$; $p<0.001$).

The calcification, maximum plaque thickness, and rad-score were incorporated into a radiomics nomogram (Fig 3a). The radiomics nomogram has a good calibration (Fig 3b). The Hosmer–Lemeshow test and the calibration curve showed good calibration in the training set ($p>0.05$), validation set ($p>0.05$), and external test set ($p>0.05$).

**Table 1**
Clinical factors of the training, validation and external test sets.

| Clinical factors | Training set (n=135) | | | Validation set (n=58) | | | External test set (n=87) | | |
|---|---|---|---|---|---|---|---|---|---|
| | Symptomatic group (n=65) | Asymptomatic group (n=70) | p-Value | Symptomatic group (n=28) | Asymptomatic group (n=30) | p-Value | Symptomatic group (n=48) | Asymptomatic group (n=39) | p-Value |
| Age, years | 63.8 ± 7.2 | 65.3 ± 8.8 | 0.259 | 63 ± 7.1 | 61 ± 8.0 | 0.327 | 62.8 ± 7.5 | 63.4 ± 8.6 | 0.742 |
| Sex, male | 52 (80) | 44 (62.9) | 0.028 | 22 (78.6) | 18 (60) | 0.127 | 38 (79.2) | 27 (69.2) | 0.289 |
| BMI, kg/m$^2$ | 25.5 ± 1.7 | 25.2 ± 1.6 | 0.211 | 25.4 ± 1.6 | 25.1 ± 1.6 | 0.420 | 25.6 ± 1.7 | 25.3 ± 1.6 | 0.496 |
| Hypertension | 56 (86.2) | 56 (80) | 0.342 | 13 (46.4) | 11 (36.7) | 0.451 | 41 (85.4) | 32 (82.1) | 0.671 |
| Hyperlipidaemia | 32 (49.2) | 216 (30) | 0.022 | 22 (78.6) | 25 (83.3) | 0.644 | 22 (45.8) | 10 (25.6) | 0.052 |
| Diabetes | 26 (40) | 23 (32.9) | 0.388 | 9 (32.1) | 11 (36.7) | 0.717 | 21 (43.8) | 9 (23.1) | 0.044 |
| Smoking | 51 (78.5) | 50 (71.4) | 0.347 | 18 (64.3) | 18 (60) | 0.737 | 36 (75) | 29 (74.4) | 0.945 |
| CAD | 40 (61.5) | 40 (57.1) | 0.604 | 13 (46.4) | 14 (46.7) | 0.986 | 30 (62.5) | 22 (56.4) | 0.565 |
| Antihypertension use | 53 (81.5) | 51 (72.9) | 0.231 | 22 (78.6) | 22 (73.3) | 0.641 | 39 (81.3) | 30 (76.9) | 0.620 |
| Statin use | 51 (78.5) | 48 (68.6) | 0.194 | 22 (78.6) | 19 (63.3) | 0.203 | 39 (81.3) | 23 (59) | 0.022 |
| Antiplatelet use | 49 (75.4) | 43 (61.4) | 0.082 | 23 (82.1) | 19 (63.3) | 0.109 | 37 (77.1) | 20 (51.3) | 0.012 |
| Calcification | 64 (98.5) | 56 (80) | <0.001 | 27 (96.4) | 23 (76.7) | 0.029 | 47 (97.9) | 30 (76.9) | 0.002 |
| Degree of luminal stenosis, % | 44 ± 17.3 | 31 ± 11.7 | <0.001 | 45.6 ± 16.4 | 29 ± 11.9 | <0.001 | 44.7 ± 17.3 | 33 ± 10.4 | <0.001 |
| Maximum plaque thickness, mm | 3.9 ± 1.2 | 2.8 ± 0.8 | <0.001 | 4.1 ± 1.1 | 2.8 ± 0.8 | <0.001 | 3.9 ± 1.2 | 2.9 ± 0.9 | <0.001 |

Continuous variables are described as mean ± standard deviation (SD), and categorical variables are presented as numbers (%).
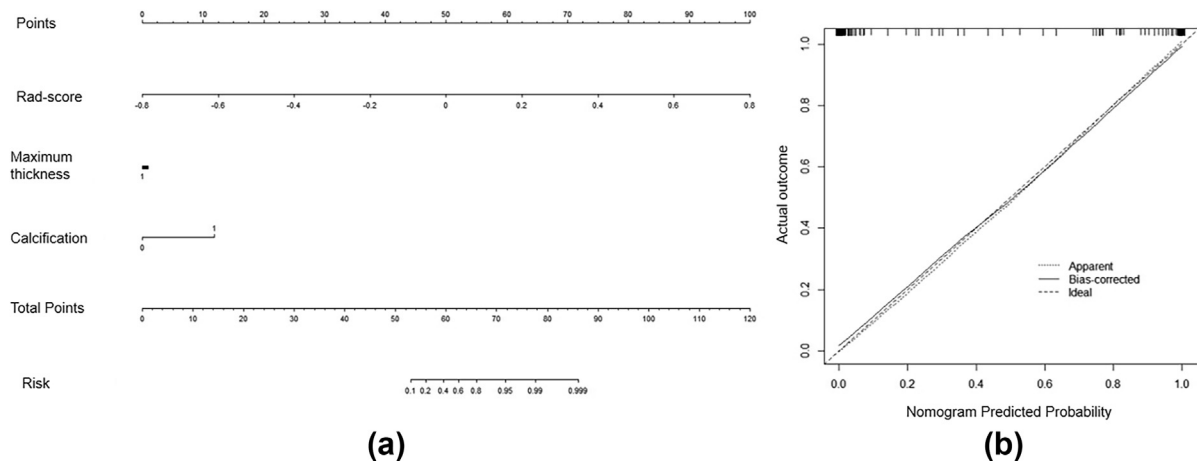BMI indicates body mass index, and CAD coronary artery disease.



**Figure 3** The radiomics nomogram and calibration curves for the radiomics nomogram. (a) The radiomics nomogram, incorporating calcification, maximum plaque thickness, and rad-score, developed in the training set. (b) Calibration curve indicates the goodness-fit of the nomogram. The 45° dotted line represents an ideal prediction, and the other dotted line represents the predictive performance of the nomogram. A closer distance between two lines indicates better prediction. The solid line indicates the deviation corrected.

**Table 2**
Diagnostic performance of three models for identification of symptomatic plaque.

| Set | Model | AUC (95% CI) | Sensitivity | Specificity | Accuracy |
|---|---|---|---|---|---|
| Training set | Clinical model | 0.845 (0.773−0.902) | 90.8% | 60% | 74.8% |
| | Radiomics signature | 0.976 (0.934−0.995) | 92.3% | 95.7% | 94.1% |
| | Radiomics nomogram | 0.981 (0.941−0.997) | 93.9% | 94.3% | 94.1% |
| Validation set | Clinical model | 0.862 (0.746−0.938) | 60.7% | 93.3% | 77.6% |
| | Radiomics signature | 0.944 (0.850−0.987) | 85.7% | 86.7% | 86.2% |
| | Radiomics nomogram | 0.977 (0.899−0.999) | 96.4% | 90% | 93.1% |
| External test set | Clinical model | 0.818 (0.721−0.892) | 52.1% | 97.4% | 72.4% |
| | Radiomics signature | 0.932 (0.857−0.975) | 91.7% | 89.7% | 90.8% |
| | Radiomics nomogram | 0.952 (0.884−0.987) | 97.9% | 87.2% | 93.1% |

AUC indicates area under the curve; CI, confidence interval.

The diagnostic performances of the clinical factor model, radiomics signature model, and radiomics nomogram are summarised in Table 2. The ROC curves of the three models are shown in Fig 4 for the training, validation, and external test cohorts. The nomogram (AUC, 0.981; 95% CI, 0.941−0.997) and radiomics signature (AUC, 0.976; 95% CI, 0.934−0.995) showed better discrimination capability ($p<0.001$ and $p<0.001$) than the clinical factor model (AUC,
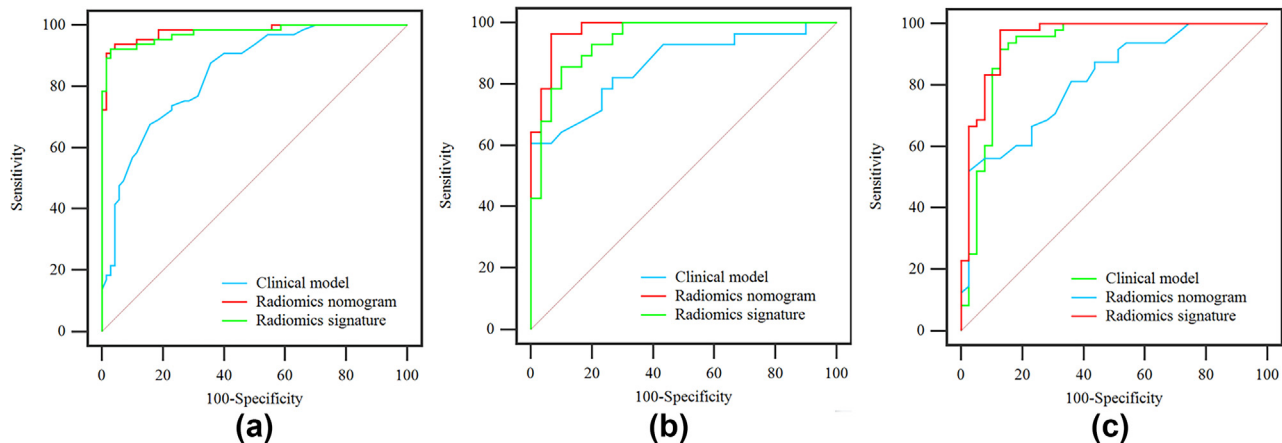
**Figure 4** The receiver operating characteristic (ROC) curves of the clinical factor model, the radiomics signature, and radiomics nomogram in the (a) training, (b) validation, and (c) external test sets, respectively. The blue line, green line, and red line represent AUCs of the clinical factors, the radiomics signature, and the radiomics nomogram, respectively.

0.845; 95% CI, 0.773−0.902) in the training set. In the validation set, the nomogram (AUC, 0.977; 95% CI, 0.899−0.999) performed better ($p=0.017$ and $p=0.031$) than the clinical factor model (AUC, 0.862; 95% CI, 0.746−0.938) and radiomics signature (AUC, 0.944; 95% CI, 0.850−0.987). In external test set, the nomogram (AUC, 0.952; 95% CI, 0.884−0.987) and radiomics signature (AUC, 0.932; 95% CI, 0.857−0.975) showed better discrimination

capability ($p=0.002$ and $p=0.037$) than clinical factor model (AUC, 0.818; 95% CI, 0.721−0.892).

The DCA for the three models is shown in Fig 5. DCA showed that the overall net benefit of the radiomics nomogram in discriminating between symptomatic and asymptomatic carotid plaques was higher than that of the clinical factor model and radiomics signature across most reasonable threshold probabilities.
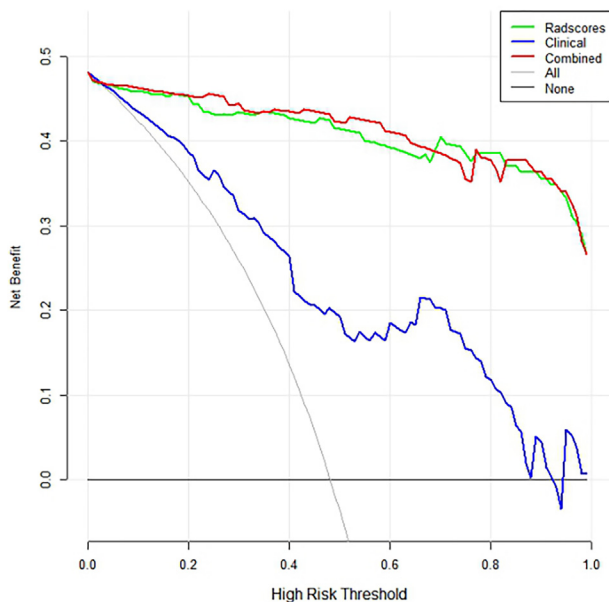


**Figure 5** Decision curve analysis for three models. The *y*-axis represents the net benefit; *x*-axis represents threshold probability. The blue line, green line, and red line indicate respectively net benefits of the three models. The grey line indicates the hypothesis that all patients had symptomatic carotid plaques. The black line indicates the hypothesis that no patients had symptomatic carotid plaques. The decision curves show that the applying nomogram to predict symptomatic carotid plaques increases more profit than the other two models.

## Discussion

The present study developed and validated a CT-based radiomics nomogram, which incorporates a radiomics signature and clinical factors for identifying high-risk carotid plaques. The radiomics nomogram showed better diagnostic performance than the clinical factor model and radiomics signature, and may act as a potential non-invasive tool to aid in the clinical diagnosis and treatment decisions for vulnerable patients.

Accurate prediction of plaque vulnerability is significant for selection of optimal therapeutic plan in patients with carotid arteriosclerosis.[15] Imaging plays a crucial role in assessing plaque vulnerability in clinical practice. Several studies have analysed the value of traditional CTA features in the identification of vulnerable plaques. Gupta *et al.*[16] showed that increasing maximum plaque thickness measurements are associated with symptomatic disease status in carotid artery stenosis, which is consistent with the present study. Several researchers found that calcification was often accompanied by intraplaque haemorrhage (IPH) and then resulted in cerebrovascular symptoms.[17] In the present study, compared with asymptomatic patients, those symptomatic patients showed a higher prevalence of calcification; however, several studies have reported that more carotid calcification was shown in asymptomatic patients with carotid plaques compared to symptomatic patients, supporting that calcification was a protective factor.[18] Sample size, examination modality, and location of

calcification may be responsible for this discrepancy. In present study, the clinical factor model based on calcification and maximum plaque thickness did not achieve a high AUC (0.845 in the training set; 0.862 in the validation set; 0.818 in the external test set). In addition, previous studies have shown measurements of stenosis can be predictive of future carotid symptoms.[19] With the development of MRI technology, several investigators have shown that compositional characteristics in carotid plaques, particularly IPH and a lipid-rich necrotic core, play a key role in plaque vulnerability[4,5,20]; however, assessing various plaque features is a subjective task, and therefore, there were more overestimated and underestimated cases. Therefore, it is still challenging to identify vulnerable plaques in clinical practice by routinely used imaging techniques. In the present study, compared to the clinical factor model, the radiomics models showed greater predictive power as indicated by higher AUC values. Therefore, the radiomics may be a useful approach to improve overall diagnostic efficiency in identifying vulnerable plaques.

Radiomics is an emerging approach to extract quantitative features to transform images into mineable data to guide clinical decision-making.[6,21] At present, research into radiomics in cardiovascular imaging has fallen behind other fields, such as oncology. There are increasing reports that radiomics can be used in the diagnosis, prognosis, and treatment of tumours.[7−9] Several studies have also applied radiomics to analyse plaque features to assess cerebrovascular risk. Zaccagna *et al.*[10] showed that CT texture analysis parameters, in particular, skewness and standard deviation, may serve as a novel risk stratification method for patients with carotid atherosclerosis. Zhang *et al.*[11] enrolled 108 patients with symptomatic plaques and 54 patients with asymptomatic plaques to identify the significant MRI radiomic features that can be applied to distinguish between symptomatic and asymptomatic carotid plaques. Shi *et al.*[22] reported that radiomic analysis of plaque texture on MRI differentiated between symptomatic and asymptomatic plaques in the basilar artery, and combining clinical and radiomics model achieved an AUC of 0.974 and accuracy of 90.5%. In addition, several studies have investigated different types of texture analysis on carotid ultrasound images and emphasised the predictive efficacy of radiomics analysis in predicting future cerebrovascular diseases in asymptomatic patients.[23,24]

Compared with previous artificial intelligence studies on identifying symptomatic plaques, there are several differences and improvements in the present study. Firstly, a CT-based radiomics nomogram was proposed by integrating the radiomics model and clinical factor model, which showed favourable predictive efficacy (AUCs of 0.981, 0.977 and 0.952 in the training, validation, and external test sets, respectively) with good calibration. In addition, more net benefits of the model for most threshold probabilities can be derived from the DCA, implying that using our nomogram to identify vulnerable carotid plaques would result in better clinical outcomes. Secondly, three-dimensional ROI analysis was performed in the present study. It is reported that three-dimensional radiomics analysis appeared to

present more heterogeneity than two-dimensional ROI and improved the discrimination accuracy.[25,26] Thirdly, CTA is a widely available imaging technique for the pretreatment assessment of patients at risk.[27,28] It offers significant advantages compared with MRI in terms of speed and availability, and it is far less operator-dependent than ultrasound.[29,30] Therefore, the choice of CTA for radiomics analysis is significant and convenient for clinical application. In addition, there were relatively more cases of symptomatic plaques in the present study than those in previous studies.

In the present study, 24 features were finally chosen for use in the radiomics analysis. Among the characteristics with a large proportion, "glrlm_RunEntropy" feature reflects the uncertainty/randomness of image information.[6] A higher value indicates more heterogeneity in the texture patterns. The present study suggested that plaques with mixed density and heterogeneous composition are more prone to the represent symptomatic plaques. The "firstorder_Mean", "firstorder_RootMeanSquared", "firstorder_Range", and "firstorder_Kurtosis" features reflect the image pixel intensity and distribution characteristics within the ROI.[6] In the present study, these features reflect the density and homogeneity of carotid plaque.

In addition, 280 individuals were analysed by segmenting the plaque, extracting radiomic features, and constructing the nomogram. For one individual, the time required to segment the plaque, extract radiomic features, and construct the nomogram is approximately 5, 3, and 1 min, respectively. Three-dimensional ROI segmentation was performed, which is complicated and time-consuming. The diagnostic efficiency and fast duration will make radiomics applications in clinic appealing.

Several limitations of the present study should be noted. First, this is a retrospective study and cannot predict subsequent ischaemic cerebrovascular events. Prospective research using the radiomics nomogram for forecasting risk stratification of carotid plaques is ongoing. Second, the study had a small sample size, and a large-scale multicentre study is required to further validate the nomogram. Third, three-dimensional ROI segmentation is complicated and time-consuming. An automatic segmentation method for carotid plaques is needed in the future.

In conclusion, the present study presented a CT-based nomogram that showed satisfactory performance in identifying high-risk plaques in carotid arteries. The radiomics nomogram may act as a non-invasive and potential tool to identify carotid plaque vulnerability and risk stratification.

## Conflict of interest

The authors declare no conflict of interest.

## Acknowledgements

## Appendix A. Supplementary data

Supplementary data to this article can be found online at https://doi.org/10.1016/j.crad.2023.07.018.

## References

1. Mozaffarian D. Global scourge of cardiovascular disease: time for health care systems reform and precision population health. *J Am Coll Cardiol* 2017;**70**(1):26–8.
2. Piepoli MF, Hoes AW, Agewall S, *et al.* 2016 European guidelines on cardiovascular disease prevention in clinical practice: the sixth joint task Force of the European society of cardiology and other societies on cardiovascular disease prevention in clinical practice (constituted by representatives of 10 societies and by invited experts)Developed with the special contribution of the European association for cardiovascular prevention & rehabilitation (EACPR). *Eur Heart J* 2016;**37**(29):2315–81.
3. Song P, Fang Z, Wang H, *et al.* Global and regional prevalence, burden, and risk factors for carotid atherosclerosis: a systematic review, meta-analysis, and modelling study. *Lancet Glob Health* 2020;**8**(5):e721–9.
4. Saba L, Saam T, Jäger HR, *et al.* Imaging biomarkers of vulnerable carotid plaques for stroke risk prediction and their potential clinical implications. *Lancet Neurol* 2019;**18**(6):559–72.
5. Saba L, Moody AR, Saam T, *et al.* Vessel wall-imaging biomarkers of carotid plaque vulnerability in stroke prevention trials: a viewpoint from the Carotid Imaging Consensus Group. *JACC Cardiovasc Imaging* 2020;**13**(11):2445–56.
6. Mayerhoefer ME, Materka A, Langs G, *et al.* Introduction to radiomics. *J Nucl Med* 2020;**61**(4):488–95.
7. Sun R, Limkin EJ, Vakalopoulou M, *et al.* A radiomics approach to assess tumour-infiltrating CD8 cells and response to anti–PD-1 or anti–PD-L1 immunotherapy: an imaging biomarker, retrospective multicohort study. *Lancet Oncol* 2018;**19**(9):1180–91.
8. Chetan MR, Gleeson FV. Radiomics in predicting treatment response in non-small-cell lung cancer: current status, challenges and future perspectives. *Eur Radiol* 2021;**31**(2):1049–58.
9. Zheng YM, Li J, Liu S, *et al.* MRI-Based radiomics nomogram for differentiation of benign and malignant lesions of the parotid gland. *Eur Radiol* 2021;**31**(6):4042–52.
10. Zaccagna F, Ganeshan B, Arca M, *et al.* CT texture-based radiomics analysis of carotid arteries identifies vulnerable patients: a preliminary outcome study. *Neuroradiology* 2021;**63**(7):1043–52.
11. Zhang R, Zhang Q, Ji A, *et al.* Identification of high-risk carotid plaque with MRI-based radiomics and machine learning. *Eur Radiol* 2021;**31**(5):3116–26.
12. McArdle PF, Kittner SJ, Ay H, *et al.* Agreement between TOAST and CCS ischaemic stroke classification: the NINDS SiGN study. *Neurology* 2018;**83**(18):1653–60.
13. Sacco RL, Kasner SE, Broderick JP, *et al.* An updated definition of stroke for the 21st century: a statement for healthcare professionals from the American Heart Association/American Stroke Association. *Stroke* 2013;**44**(7):2064–89.
14. North American Symptomatic Carotid Endarterectomy Trial Collaborators, Barnett HJM, Taylor DW, Haynes RB, *et al.* Beneficial effect of carotid endarterectomy in symptomatic patients with high-grade carotid stenosis. *N Engl J Med* 1991;**325**(7):445–53.
15. Spanos K, Tzorbatzoglou I, Lazari P, *et al.* Carotid artery plaque echo-morphology and its association with histopathologic characteristics. *J Vasc Surg* 2018;**68**(6):1772–80.
16. Gupta A, Baradaran H, Kamel H, *et al.* Evaluation of computed tomography angiography plaque thickness measurements in high-grade carotid artery stenosis. *Stroke* 2014;**45**(3):740–5.
17. Lin R, Chen S, Liu G, *et al.* Association between carotid atherosclerotic plaque calcification and intraplaque hemorrhage: a magnetic resonance imaging study. *Arterioscler Thromb Vasc Biol* 2017;**37**(6):1228–33.
18. Kwee RM. Systematic review on the association between calcification in carotid plaques and clinical ischaemic symptoms. *J Vasc Surg* 2010;**51**(4):1015–25.
19. Fairhead JF, Rothwell PM. The need for urgency in identification and treatment of symptomatic carotid stenosis is already established. *Cerebrovasc Dis* 2005;**19**(6):355–8.
20. Zhu G, Hom J, Li Y, *et al.* Carotid plaque imaging and the risk of atherosclerotic cardiovascular disease. *Cardiovasc Diagn Ther* 2020;**10**(4):1048–67.
21. Wang Y, Liu W, Yu Y, *et al.* CT radiomics nomogram for the preoperative prediction of lymph node metastasis in gastric cancer. *Eur Radiol* 2020;**30**(2):976–86.
22. Shi Z, Zhu C, Degnan AJ, *et al.* Identification of high-risk plaque features in intracranial atherosclerosis: initial experience using a radiomic approach. *Eur Radiol* 2018;**28**(9):3912–21.
23. Kyriacou EC, Petroudi S, Pattichis CS, *et al.* Prediction of high-risk asymptomatic carotid plaques based on ultrasonic image features. *IEEE Trans Inf Technol Biomed* 2012;**16**(5):966–73.
24. van Engelen A, Wannarong T, Parraga G, *et al.* Three-dimensional carotid ultrasound plaque texture predicts vascular events. *Stroke* 2014;**45**(9):2695–701.
25. Guo Y, Chen X, Lin X, *et al.* Non-contrast CT-based radiomic signature for screening thoracic aortic dissections: a multicentre study. *Eur Radiol* 2021;**31**(9):7067–76.
26. Nie P, Yang G, Wang Z, *et al.* A CT-based radiomics nomogram for differentiation of renal angiomyolipoma without visible fat from homogeneous clear cell renal cell carcinoma. *Eur Radiol* 2020;**30**(2):1274–84.
27. Chrencik MT, Khan AA, Luther L, *et al.* Quantitative assessment of carotid plaque morphology (geometry and tissue composition) using computed tomography angiography. *J Vasc Surg* 2019;**70**(3):858–68.
28. Knight-Greenfield A, Quitlong Nario JJ, Vora A, *et al.* Associations between features of nonstenosing carotid plaque on computed tomographic angiography and ischemic stroke subtypes. *J Am Heart Assoc* 2019;**8**(24):e014818.
29. Ospel JM, Singh N, Marko M, *et al.* Prevalence of ipsilateral nonstenotic carotid plaques on computed tomography angiography in embolic stroke of undetermined source. *Stroke* 2020;**51**(6):1743–9.
30. Brinjikji W, Huston 3rd J, Rabinstein AA, *et al.* Contemporary carotid imaging: from degree of stenosis to plaque vulnerability. *J Neurosurg* 2016;**124**(1):27–42.